Ecotoxicology and Environmental Safety 303 (2025) 118862

Contents lists available at ScienceDirect

Ecotoxicology and Environmental Safety

journal homepage: www.elsevier.com/locate/ecoenv

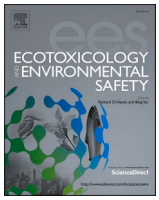

Gas bubble trauma of *Schizothorax prenanti* at various life stages induced by total dissolved gas supersaturation

Quan Yuan [a,b], Jun Du [c], Kefeng Li [b], Bo Zhu [a], Ruifeng Liang [b], Yuanming Wang [b,*]

[a] School of Agriculture and Biology, Shanghai Jiao Tong University, Shanghai 200240, China
[b] State Key Laboratory of Hydraulics and Mountain River Engineering, Sichuan University, Chengdu 610065, China
[c] The Fishery Institute of the Sichuan Academy of Agricultural Sciences, Chengdu, 611730, China

ARTICLE INFO

Keywords:
Total dissolved gas supersaturation
Early development
Gas bubble trauma
Metabolic rates
Swimming performance

ABSTRACT

Total dissolved gas supersaturation (TDGS), commonly resulting from dam discharge, poses significant threats to fish survival by inducing gas bubble trauma (GBT) in downstream populations. Understanding the sensitivity of fish to TDGS during developmental stages is critical for evaluating survival risks during flood seasons. This study investigated the adverse effects of TDGS on three life stages—eggs, larvae, and juveniles—of the endemic fish *Schizothorax prenanti* (*S. prenanti*) in the upper Yangtze River. After hatching in 120 % and 130 % TDG levels, both eggs and larvae exhibited severe GBT symptoms with survival rates declining to 70 % and 77 % respectively, compared to 88 % in the control group. Hatching rates also dropped significantly to 66 % and 59 %, compared to 84 % in the control group. Larvae exhibited a marked reduction in body length at TDG levels above 120 %, while heart rates increased significantly at TDGS levels above 110 %. Juveniles subjected to 120 % and 130 % TDGS showed extensive GBT symptoms, with median lethal times of 92 and 35 h, respectively. After 35 h of exposure, juveniles in the 130 % TDGS group showed significant reductions in active metabolic rate (AMR), standard metabolic rate (SMR), and factorial aerobic scope (F-AS), while critical swimming speed (U_{crit}) and burst swimming speed (U_{burst}) remained unchanged compared to the control group. In terms of *S. prenanti* exposed to 130 % TDGS, U_{crit} and U_{burst} significantly declined when survival rate dropped to 25 %, while AMR, SMR, and F-AS exhibited significant changes prior to mortality occurred. Moreover, AMR, SMR, and F-AS in juveniles were more vulnerable to TDGS than U_{crit} and U_{burst}. These findings enhance the understanding of TDGS-induced stress on developing fish and support the development of ecological management strategies for TDG during flood seasons.

1. Introduction

Hydropower serves as a crucial renewable energy source that facilitates flood control, navigation, irrigation, and water supply, while also contributing to energy conservation, emission reductions, thus addressing the global energy crisis (Grill et al., 2019; Latrubesse et al., 2017). However, the construction of dams has profoundly impacted riverine ecosystems, leading to altered hydraulic conditions, habitat fragmentation, and the emergence of total dissolved gas supersaturation (TDGS) (Pulg et al., 2024; Yang et al., 2024). These environmental changes have resulted in declines in wild fish populations and a significant reduction in biodiversity (Huang and Li, 2024). Among the various environmental threats posed by dams, TDGS is particularly concerning during flood seasons. Discharge flow from hydropower facilities always take large amount of air into downstream river. Since gas solubility increases with water depth and hydrostatic pressure, entrained air can be totally dissolved under high pressure within downstream energy dissipation pool (Berg, 1992; Li et al., 2022; Pulg et al., 2016). When this water subsequently flows into shallower areas or surfaces, pressure is relieved, causing TDG levels to exceed 100 %. The excess gas forms bubbles and degasses slowly, but supersaturation persists during this re-equilibration process. This slow dissipation process may take a longer time duration and may affect dozens of kilometers of the river downstream (Pulg et al., 2024).

This TDGS water is continuously produced by dam releases during flood events, and can travel downstream for several kilometers, with gas gradually dissipating along the river (Li et al., 2022). Fish inhabiting these affected river sections are particularly vulnerable to TDGS, often

* Corresponding author.
E-mail address: wangyuanming1991@126.com (Y. Wang).

https://doi.org/10.1016/j.ecoenv.2025.118862
Received 13 April 2025; Received in revised form 9 August 2025; Accepted 10 August 2025
Available online 12 August 2025

suffering from gas bubble trauma (GBT), which adversely impacts their reproduction, growth, and swimming behavior, and causes acute mortality in severe cases (Pleizier et al., 2020). The Yangtze River basin was a global hotspot for research on TDGS impacts on fish (Pleizier et al., 2020), primarily due to the high levels of TDGS generated by its large dams and the extensive effects of cascade hydropower operations. Additionally, the basin's rich diversity of endemic fish species, coupled with their unique ecological value, underscored the urgent need for targeted conservation efforts.

Survival and development of fish eggs and larvae have specific environmental requirements, such as temperature, flow rate and dissolved oxygen, among others (Stuart and Sharpe, 2020). Numerous studies indicated that human activities, particularly hydroelectric dam construction, have significantly influenced these critical habitats. Dams contribute to the loss of spawning and nursery grounds, impairing fish reproduction (Sanches et al., 2006; Zhang et al., 2021), which in turn affects fish populations. The primary impacts of dams on fish eggs include alterations in water temperature, hydraulic conditions, and TDGS (Chen et al., 2023a).

Previous research underscored the heightened vulnerability of fish eggs to TDGS. For instance, salmon eggs required chronic exposure levels below 104–105 % TDGS to ensure normal hatching in surface waters, with acute exposure levels not exceeding 109–110 % TDGS (Arntzen et al., 2009). In TDGS-affected waters, *Salvelinus namaycush* eggs have been observed to perish prior to hatching, demonstrating complete absorption of their yolk sacs (Krise and Herman, 1989). Field studies indicated that certain species, such as salmon, preferentially spawn in hydropower tailwaters, thereby compelling their eggs to hatch in TDGS-rich environments (Arntzen et al., 2009; Weitkamp and Katz, 1980). Migratory fish in the upper Yangtze River, whose migration periods coincide with peak TDGS levels, were particularly susceptible to these detrimental effects (Liang et al., 2013). The hatching success of endemic species in the upper Yangtze, including *Schizothorax davidi* and *Myxocyprinus asiaticus Bleeker*, has also been adversely affected by TDGS (Li et al., 2019; Liang et al., 2013). Despite of the well-documented impacts of TDGS on fish egg hatching, limited research has addressed its influence on early larval development.

Energy metabolism is fundamental to fish, underpinning all biological processes and intricately interacting with the organism's physiology and ecology (Mommsen, 1998). Oxygen consumption (MO_2) serves as a critical indicator of metabolic activity and is frequently measured alongside critical swimming speed (U_{crit}) (Messina-Henríquez et al., 2022). Fish physiologists utilize swimming respirometry to evaluate metabolic capacities, including the standard metabolic rate (SMR)—the minimum energy expenditure of unfed fish at rest—and the active metabolic rate (AMR), which reflects the energy demand of fish swimming at their maximum sustainable speed during U_{crit} trials (Hanna et al., 2021). The factorial aerobic scope (F-AS) quantifies the ratio of AMR to SMR. Variations in MO_2 can signal stress in fish, and environmental stressors such as salinity and temperature have been shown to influence both metabolic consumption and swimming energy expenditure (Glover et al., 2012). Previous research suggested that GBT could damage fish gills and other respiratory systems. Additionally, the accumulation of microbubbles caused by GBT in blood vessels might block the circulatory system, both indicating potential adverse effects of TDG on energy metabolism. Although the correlation between metabolic capacity and swimming performance was established, the direct effects of TDGS on fish metabolic processes and their subsequent influence on swimming ability remain unclear.

Schizothorax prenanti (*S. prenanti*) plays a crucial role in riverine food web stability by grazing on benthic algae and serving as a key prey species for large predatory fish such as sturgeons. Its primary habitats—rivers like the upper Yangtze, Lancang, and Jinsha—are vital freshwater ecosystems, rich in endemic fish diversity and crucial for hydropower development in China. As a species highly sensitive to environmental changes, *S. prenanti* is an ideal representative for assessing the ecological risks of TDGS in endemic species. This study seeks to bridge these gaps by examining the detrimental effects of TDGS on *S. prenanti* across various life stages, including egg hatching, larval development, and juvenile survival. By exploring physiological aspects such as swimming performance and energy metabolism, this research aims to provide a comprehensive understanding of TDGS-induced stress, contributing to the development of ecological management strategies for the conservation of this species during flood seasons. This research provides valuable insights for balancing hydropower development with ecological conservation, contributing to the long-term preservation of aquatic biodiversity.

2. Materials and methods

2.1. Embryo and juvenile fish

Three developmental stages of *S. prenanti*, including embryos, larvae, and juveniles, were examined in this study. The embryos refer to the stage from 24 h post-fertilization until the hatching period. The larvae refer to the stage from 48 h post-hatching until the hatching period. The juveniles refer to the stage at approximately 6 months post-hatching. Eggs and juveniles of *S. prenanti* were obtained from the Dadu River Company hatchery. For experimental purposes, only successfully fertilized eggs were selected. Upon arrival at the laboratory, the eggs were maintained for 24 h in a controlled environment with continuously oxygenated, flowing freshwater facilitated by multiple tank overflows. Freshwater used in this study was dechlorinated tap water, which had a water temperature of 17 ± 0.5°C, a pH range of 6.8–7.2, and a dissolved oxygen (DO) level above 5 mg/L. Prior to TDGS exposure, white eggs with opaque or partially opaque membranes were removed, and healthy eggs were systematically grouped.

Juvenile fish were transported to the laboratory using a similar procedure. Upon arrival, they were placed in static freshwater tanks where continuous aeration was maintained, this constituted a three-day acclimation period (Wang et al., 2024; Zhang et al., 2024). The water used for juvenile holding, consistent with that employed in the subsequent juvenile experiments, was dechlorinated tap water. During this period, *S. prenanti* were fed commercial feed (Tongwei Special Feed for *S. prenanti*) twice a day, and one-third of the tank water was replaced each day. Juvenile fish were not fed for 24 h before the experiment. The water conditions during juvenile acclimation were consistent with those employed during the egg acclimation phase. A 14:10 h light-dark photoperiod was established for both embryonic incubation and juvenile holding.

2.2. TDGS generation and monitoring

Water was drawn from the tank into the autoclave using a pump, while a compressor supplied the necessary compressed gas. Within the autoclave, high-TDGS water was generated by mixing the water with the compressed gas. A valve was employed to control the ratio of high-TDGS water to equilibrated water, thereby achieving the desired TDGS level for the experiment. A detailed explanation of the TDGS water generation system was provided by (Wang et al., 2018). Throughout the experiments, TDGS levels were continuously monitored using the Point Four Tracker (Point Four Systems Inc., Canada). The TDG measurement tool was calibrated prior to use, reaching atmospheric pressure equilibrium when exposed to air. Calibration was completed by pressing the corresponding button. Before measuring TDG, the probe was placed in equilibrium water to obtain a 100 ± 1 % reading. A stable reading was achieved by gently moving the probe in the top layer of TDG-supersaturated water for 3–5 min. Water temperature was recorded with a ZDR temperature recorder (Zheda Inc., China), and DO concentration was measured using a multiparameter water quality sonde (NCL of Wisconsin, Inc., USA). The DO device is calibrated by immersing the sensor in an oxygen-free environment for zero-point

calibration and using a standard solution with a known concentration (such as a saturated oxygen solution) for the standard calibration. The water temperature and pH during the exposure phase were maintained similar to those in the acclimation phase. Water temperature was recorded with a ZDR temperature recorder (Zheda Inc., China), ranging from 16 to 18 ℃ during the experiment phase.

2.3. Experimental method

2.3.1. Experimental design for larvae

Hatching containers were constructed from 10 cm diameter plexiglass tubes with fine mesh bottoms (Fig. 1(b)) and placed within a rectangular plexiglass channel measuring 200 cm × 15 cm × 15 cm (Fig. 1(a)). A baffle was installed at the downstream to effectively control the water depth, helping to submerge the eggs in 8 cm of flowing water (Fig. 1(b)). Four channels were supplied with water at TDGS levels of 100 % (control), 110 %, 120 %, and 130 %. Each channel contained three hatching containers, serving as parallel samples, with each container holding 200 eggs. The eggs remained in flowing water at their corresponding TDGS levels for about a week until hatching. During the hatching period, the eggs were monitored twice daily, in the morning and afternoon, with non-viable eggs promptly removed to prevent mould from affecting healthy eggs.

Typical GBT symptoms in eggs and newly hatched larvae during the hatching period were systematically observed and documented using a stereo microscope (Olympus-SZ61, Japan). After hatching, the numbers of hatched and non-viable individuals in each container were recorded to calculate the hatching and morality rates. The hatching rate was determined by dividing the number of hatched larvae by the total number of embryos and larvae. A total of 30 larvae were randomly selected from 3 incubators for heart rate measurement. Larvae were processed individually to ensure timely assessment. Each larva was transferred to a glass Petri dish and anesthetized in 0.01 % MS-222 (Sigma, USA). The heart rate of each larva was determined by counting beats for 1 min under real-time observation using a stereo microscope. The procedure, including heartbeat counting, was completed within 3 min since removal from the incubator. All observations were simultaneously video-recorded to enable subsequent verification of heart rate counts through video review. The total body length of larval was measured from the tip of the snout to the distal end of the longest caudal fin ray using stereo-microscopy.

2.3.2. Experimental design for juveniles

The TDGS exposure setup for juveniles consists of a 200 cm × 15 cm × 15 cm plexiglass channel. Water enriched with TDGS was pumped from a reservoir into the upstream end of the channel, with the flow rate manually regulated via a valve to maintain a steady and slow water flow. To ensure a consistent water depth, a plexiglass plate was placed at the downstream, maintaining the depth at 12 cm. The exposure area for the fish was a 1-meter section located in the middle of the channel, separated by two perforated plexiglass plates. The top of this section was covered with a plexiglass plate to prevent the fish from escaping (Fig. 1(c)).

To investigate the survival characteristic of juveniles in TDGS water, two replicate exposure channels were established for each TDGS level and each contained 15 fish. The exposure process lasted 96 h. Throughout the experiment, abnormal behaviors of fish were closely monitored. When exhibiting signs of impending death such as floating on the surface or remaining near the downstream perforated plate, fish were gently prodded with a small stick. If there was no response after three prods, the fish was deemed death, and the time of death was recorded accordingly. Typical GBT symptoms were photographed and documented. Additionally, the weight and fork length (from the anterior tip of the body to the median fork of the caudal fin) of each fish were measured and recorded using an electronic balance and a ruler (Table 1).

Four TDGS levels (100 %, 110 %, 120 %, and 130 %) were set to investigate the effects of various TDGS levels on the swimming performance of juvenile fish. Four fish were placed into each TDG group for 35 h, and then one of remaining fish were randomly selected and transferred to the swim chamber to measure U_{crit} and AMR (or U_{burst} or SMR). This process was repeated 6 times, aiming to get 6 replicates for each TDG group. The median lethal time of juvenile at 130 % TDGS was 35 h, we chose it as the exposure time to ensure at least half fish could survive. After testing, the body length and weight of each fish were meticulously recorded, as detailed in Table 1.

Six TDGS exposure durations were established to assess the impact of exposure duration on swimming performance. Exposure durations were set based on critical time points for juvenile fish under 130 % TDGS exposure, including start of exposure (T_1), death onset (T_3), the middle time between T_1 and T3 (T_2), 75 % survival (T_4), 50 % survival (T_5), and 25 % survival (T_6). Four fish were exposed to 130 % TDGS for each duration, and one of them was randomly selected to measure U_{crit} and AMR (or U_{burst} or SMR). This procedure was repeated six times independently for each exposure duration to obtain six replicates. Following these evaluations, the body length and weight of each fish were documented, as shown in Table 2.

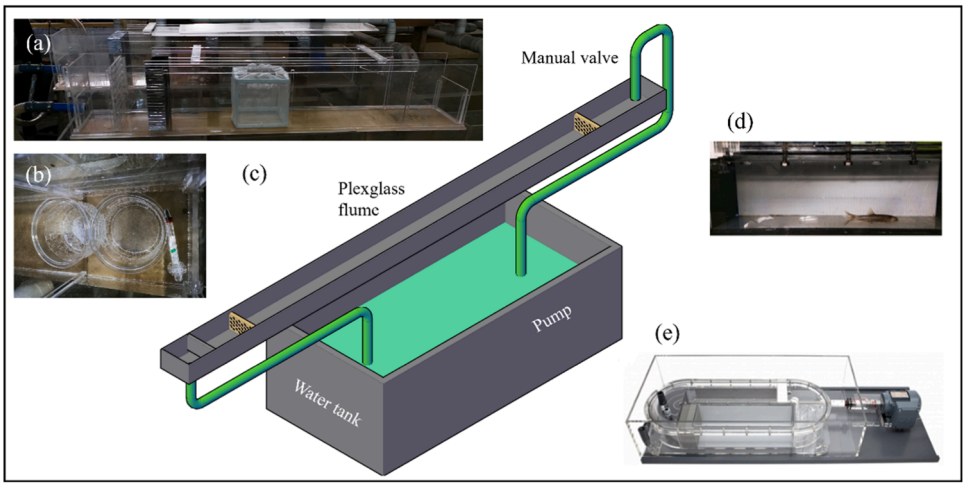

Fig. 1. Experimental setup: (a) TDGS exposure channel for fish eggs and juveniles, (b) fish egg incubator, (c) schematic diagram of the TDGS exposure channel, (d) experimental juvenile fish, (e) apparatus for testing swimming ability and dissolved oxygen (swim chamber).

Table 1
Detailed information regarding *S. prenanti* exposed to various TDGS levels. Data of length and weight are shown as mean ± standard error (SE).

	TDGS level (%)	Number of fish	Fork length (cm)	Weight (g)
Survival and GBT	100	30	8.5 ± 0.7	6.3 ± 1.3
	110	30	8.4 ± 0.4	6.1 ± 1.6
	120	30	8.8 ± 1.1	6.7 ± 1.8
	130	30	8.1 ± 0.7	5.9 ± 1.4
U_{crit} and AMR	100	6	9.3 ± 1.1	7.0 ± 2.0
	110	6	8.3 ± 0.9	6.5 ± 1.9
	120	6	8.2 ± 0.5	5.2 ± 1.3
	130	6	8.4 ± 0.4	5.2 ± 1.3
U_{burst}	100	6	8.8 ± 0.9	6.7 ± 2.4
	110	6	8.9 ± 0.7	6.5 ± 2.1
	120	6	8.3 ± 0.6	5.4 ± 1.1
	130	6	8.2 ± 0.8	5.6 ± 2.1
SMR	100	6	8.6 ± 0.4	6.5 ± 1.4
	110	6	8.2 ± 0.8	5.8 ± 1.3
	120	6	8.3 ± 1.6	5.9 ± 1.1
	130	6	8.7 ± 0.5	6.4 ± 1.4

Table 2
Details on *S. prenanti* exposed to 130 % TDGS for various durations. Data of length and weight are shown as mean ± SE.

	Survival rate (%)	Exposure duration	Number of fish	Fork length (cm)	Weight (g)
U_{crit} and AMR	100	T_1	6	8.3 ± 0.5	6.0 ± 1.3
	100	T_2	6	8.1 ± 0.4	5.8 ± 1.5
	100	T_3	6	8.0 ± 0.4	5.2 ± 1.0
	75	T_4	6	7.9 ± 0.5	5.2 ± 1.5
	50	T_5	6	8.2 ± 0.2	5.5 ± 1.0
	25	T_6	6	7.9 ± 1.0	5.7 ± 1.5
U_{burst}	100	T_1	6	8.5 ± 0.5	6.3 ± 1.0
	100	T_2	6	8.2 ± 0.7	6.5 ± 1.9
	100	T_3	6	7.9 ± 0.5	5.2 ± 0.8
	75	T_4	6	7.7 ± 0.9	5.5 ± 2.0
	50	T_5	6	7.8 ± 0.6	4.7 ± 1.2
	25	T_6	6	8.1 ± 0.3	5.0 ± 1.1
SMR	100	T_1	6	8.3 ± 0.6	6.3 ± 0.8
	100	T_2	6	7.9 ± 0.7	5.7 ± 1.7
	100	T_3	6	8.1 ± 1.2	5.9 ± 1.4
	75	T_4	6	8.6 ± 0.4	6.4 ± 0.6
	50	T_5	6	8.2 ± 0.8	6.3 ± 1.4
	25	T_6	6	8.0 ± 0.7	5.5 ± 1.4

2.3.3. Measurement of SMR, AMR, F-AS, U_{crit} and U_{burst} for juveniles

To assess the swimming performance and metabolic rates of the fish, a flume-type swimming respirometer (SW10200, Loligo Systems, Denmark) with a 90 L capacity and a 28 L rectangular swim chamber was utilized. The respirometer was submerged in the tank (Fig. 1(e)), equipped with a temperature sensor and a dissolved oxygen microsensor inserted into the left section of the swim chamber. Witrox oxygen meter was employed to measure temperature and oxygen levels in real-time, while AutoResp software was used to calculate MO_2. The Witrox oxygen meter measured temperature and oxygen levels in real-time, and AutoResp software was used to calculate MO_2. Flow measurements were conducted using a handheld flow meter, consisting of a main unit. Prior to the experiment, the probe was placed vertically in the center of the swimming test area, with its rotating blades positioned in the mid-water layer. Flow speed measurements were conducted using the flow meter, and the system was calibrated based on the established linear relationship between propeller speed and water flow speed.

SMR is defined as the minimum sustainable level of MO_2 at a specific temperature (Chabot et al., 2016). Farrell (2016) described various experimental conditions and methods for measuring SMR. A frequently employed method involves placing fish within a respirometer under conditions conducive to calm inactivity, without the concurrent measurement of locomotor activity (Farrell, 2016). This simple and cost-effective method was adopted in this study.

For this study, the swim chamber was submerged in a large, continuously aerated tank. Before measuring SMR, AMR, U_{crit}, and U_{burst}, the water in the swim tunnel was replaced with oxygen-saturated water from the large tank using a pump. Once the juveniles exposed to TDGS were transferred into the swim chamber, the pump was turned off, and the chamber was sealed. After a 30-minute acclimation in the stationary swim chamber (with a flow rate of 0), a 1-hour dissolved oxygen decline curve was generated using an oxygen probe and AutoResp software. The SMR was calculated by dividing the change in dissolved oxygen over the 1-hour period by the fish's body weight and time.

The U_{crit} test offers a standardized evaluation of prolonged swimming ability, following the methodology of Brett (1964). In this study, juveniles exposed to TDGS were acclimated for 30 min at a water flow speed equivalent to half their body length per second. Subsequently, the flow speed was incrementally increased by an additional body length per second every 15 min until the point of exhaustion was reached. U_{crit} was calculated using the following equation:

$$U_{crit} = V_1 + (t/T) \times V_2 \quad (1)$$

where T represents the time allocated to swim at each speed (15 min), V_1 denotes the maximum speed sustained by the fish for the entire period (in body lengths per second, BL/s), V_2 is the incremental velocity increase (1 BL/s), and t (in minutes) is the duration the fish swam at the final speed.

In this experiment, AMR was calculated by dividing the difference in oxygen consumption before and after the U_{crit} test by time and body weight. F-AS was then determined by dividing AMR by SMR. The U_{burst} test was conducted in a manner similar to the U_{crit} test, with water flow speed increasing by 1 BL/s every 20 s until the fish reached exhaustion in the swim chamber.

2.4. Statistical analysis

Data were collected on egg hatchability and mortality, larval total

length and heartbeat, as well as juvenile SMR, AMR, FAS, U_{crit} and U_{burst}. For datasets concerning juvenile swimming abilities (SMR, AMR, FAS, U_{crit} and U_{burst}.) that met the assumption of normality (verified using the Shapiro-Wilk test with $p > 0.05$), interspecies differences were tested using one-way ANOVA. When the normality assumption was violated, the non-parametric Kruskal-Wallis test was used. Significant results from these tests were followed by post hoc multiple comparisons using Dunnett's test with Bonferroni correction to control family-wise error rates. Statistical significance for multiple comparisons was determined using Bonferroni-adjusted p-values. Data are presented as mean ± SE.

The effects of TDGS level, exposure duration, and survival rate on the U_{crit} and U_{burst} of juveniles were analyzed using R software (R Core Team, 2023). Separate multiple linear regression models were fitted for U_{crit} and U_{burst} as dependent variables, using the lm () function. The predictor variables included TDGS (%), duration (hours), and survival rate (%). Prior to model selection, key assumptions of linear regression were validated. Linearity between predictors and each response variable was confirmed using component-plus-residual plots. Homoscedasticity of residuals was verified via scale-location plots and Breusch-Pagan tests ($p > 0.05$). Normality of residuals was assessed using Shapiro-Wilk tests ($p > 0.05$) and Q-Q plots. Absence of multicollinearity among predictors was confirmed by Variance Inflation Factors. Model selection was performed using stepwise backward elimination based on the minimum Akaike Information Criterion (AIC). The general form of the final fitted models is:

$$h(t) = b_0 + b_1x_1 + b_2x_2 \ldots\ldots\ldots b_ix_i \quad (2)$$

where h represents the hazard rate of the event, the variables $x_1,\ldots, x_i$ denote the factors influencing the event, and the coefficients $b_1,\ldots, b_i$ quantify the impact of each factor.

3. Results

3.1. Impact of TDGS on S. prenanti larvae

Exposure to elevated TDGS levels significantly affected the survival and hatching rates of *S. prenanti* larvae. Specifically, the survival rates significantly decreased to 70 % and 77 % in the 120 % and 130 % TDGS groups, respectively, compared to the average 88 % in the control group (Fig. 2(a)). Similarly, the hatching rates declined to 66 % and 59 % in the 120 % and 130 % TDGS groups, respectively, both markedly lower than 84 % of the control group (Fig. 2(b)). GBT was observed in both fish eggs and larvae exposed to 130 % TDGS (Fig. 2(d)). The incidence of GBT averaged 4 % in the 120 % TDGS group and increased to 10 % in the 130 % TDGS group (Fig. 2(c)).

Larvae in the 120 % TDGS group exhibited a significant reduction in body length to 10.8 mm, and those in the 130 % TDGS group decreased to 10.7 mm, compared to 11.5 mm in the control group (Fig. 3(a)). Heart rates were also influenced by exposure to TDGS, with average rates of 112, 123, and 132 beats per minute for the 110 %, 120 %, and 130 % exposure groups, respectively, all exceeding the control group's average of 108 beats per minute (Fig. 3(b)).

3.2. Survival characteristics of juveniles

Juveniles exposed to elevated TDGS levels exhibited typical GBT symptoms, particularly in the 120 % and 130 % TDGS groups (Fig. 4(a)). No GBT symptoms were detected in the 100 % and 110 % TDGS groups. However, the prevalence and severity of bubble disease were more pronounced in the 130 % TDGS group compared to the 120 % group (Fig. 4(b)). Following 96 h of acute exposure, no mortality was recorded in the 100 % and 110 % TDGS groups. In contrast, the average semi-lethal times were 92 h for the 120 % TDGS group and significantly reduced to 35 h for the 130 % TDGS group (Fig. 4(c)).

3.3. The swimming performance of juveniles

As the TDGS level increases, both U_{crit} and U_{burst} exhibit a declining trend. (Fig. 5(a) and 5(b)). As TDGS levels increased, a decline in AMR were observed, with the 130 % TDGS group exhibiting a significant reduction to 72 % of the control group (Fig. 5(c)). Conversely, SMR of the 110 % TDGS group significantly rose to 186 % of the control group, whereas in the 130 % TDGS group, it significantly decreased to 90 % of the control group (Fig. 5(d)). The F-AS values for the 110 %, 120 %, and 130 % TDGS groups were 0.82, 0.97, and 1.27, respectively, compared to the control group's F-AS of 1.53, (Fig. 5(e)).

The U_{crit} exhibited a significant decline with extended exposure to 130 % TDGS, decreasing from 12.2 BL/s at T_1 to 5.4 BL/s at T_6 (Fig. 6(a)). Similarly, U_{burst} declined over exposure time, with a notable reduction from 13 BL/s at T_1 to 9.8 BL/s at T_6 (Fig. 6(b)). The AMR initially increased, reaching peak values of 114 % and 121 % at T_2 and T_3, respectively, before undergoing a significant decline to 69 % at T_6 (Fig. 6(c)). The SMR showed a marked decline, falling to 89 %, 83 %,

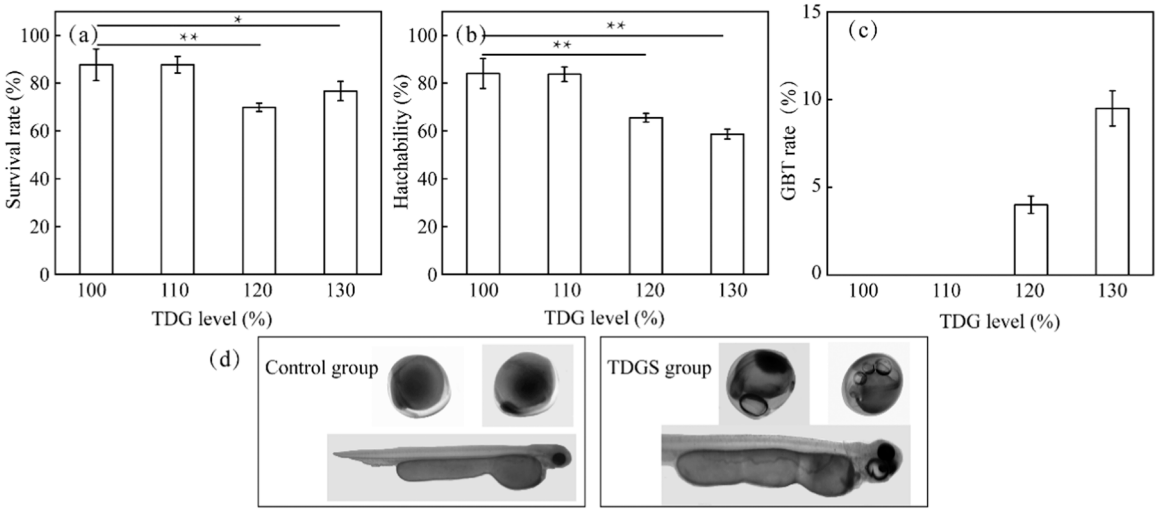

Fig. 2. The impact of exposing embryos to hatching conditions at 100 %, 110 %, 120 %, and 130 % TDGS levels. (a) Survival rate, (b) hatchability, (c) GBT incidence. n = 3. Asterisks denote the significance of the differences, with * and ** representing p-values less than 0.05 and 0.01, respectively. (d) representative images of GBT in embryos or larvae during exposure in the 120 % and 130 % TDGS groups.

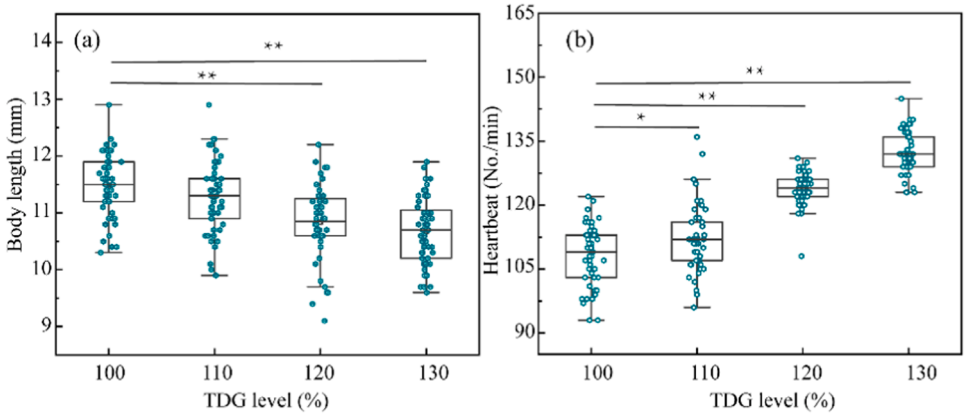

Fig. 3. The influence of TDGS levels at 100 %, 110 %, 120 %, and 130 % on the development of larval fish. (a) Body length and (b) heartbeat. n = 3. Asterisks denote the significance of the differences, with * and ** representing p-values less than 0.05 and 0.01, respectively.

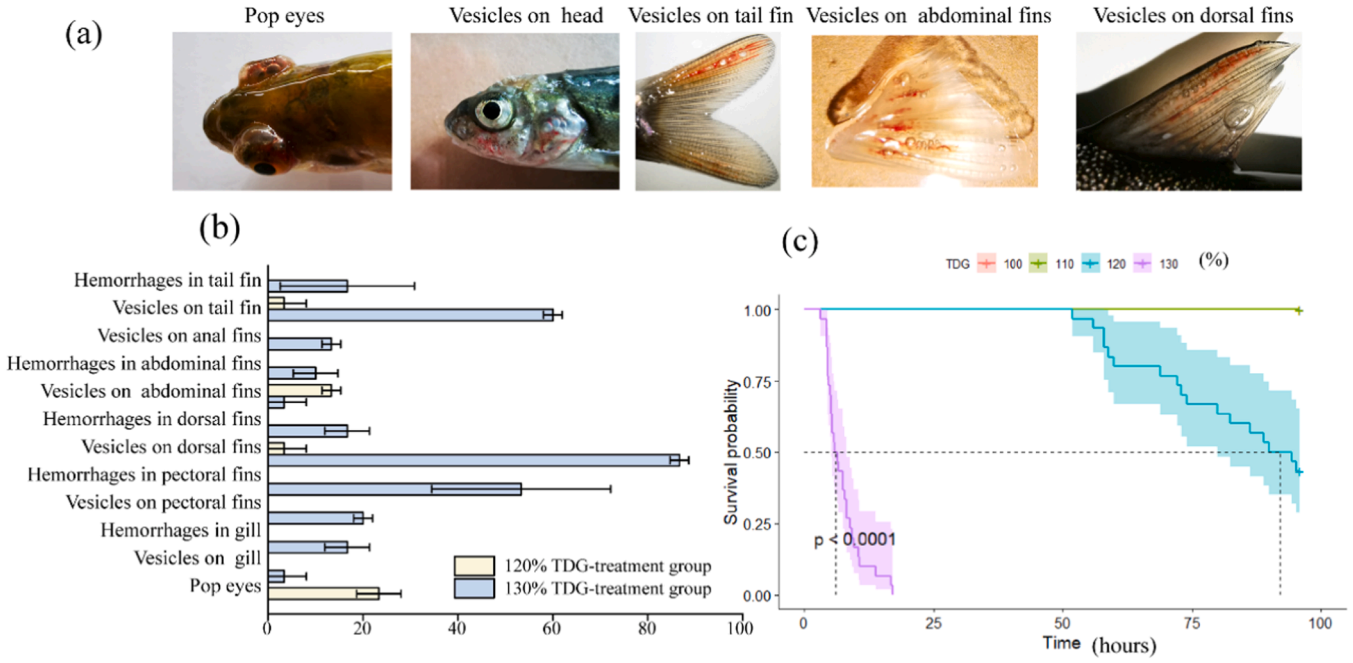

Fig. 4. The effects of TDGS exposure on juvenile fish. (a) Typical symptoms of GBT, (b) GBT prevalence, and (c) survival curves for juveniles in the 120 % and 130 % TDGS exposure groups over 96 h.

and 69 % of the control group at T_2, T_5, and T_6, respectively (Fig. 6(d)). The F-AS increased significantly from 1.06 at T_1 to 1.35 at T_2, 1.62 at T_3, and subsequently decreased to 1.28 at T_5 (Fig. 6(e)).

The analysis of U_{crit} involved four selected models, as detailed in Table 3. Model 2, which integrated both TDGS level and survival rate (AIC 295), exhibited the best fit to the data. Adding exposure duration did not enhance this model (AIC 297). The relationship between U_{crit}, TDGS level, and survival rate was evaluated using the following multiple linear regression model:

$$U_{crit} = 19.01 - 10.42 \times TDGS + 7.57 \times Survival\ rate. \quad (3)$$

Similarly, the four selected models for analyzing U_{burst} are presented in Table 4. Model 2, which incorporates both TDGS level and survival rate (AIC 256), demonstrated the best fit to the data. The inclusion of exposure duration did not improve this model's performance (AIC 258). The relationship between U_{burst}, TDGS level, and survival rate was evaluated using the following multiple linear regression model:

$$U_{burst} = 15.09 - 3.77 \times TDGS - 2.75 \times Survival\ rate. \quad (4)$$

4. Discussion

4.1. The effect of TDGS on embryos and larvae

In this study, substantial bubble formation was evident on the eggs and fry of *S. prenanti*. Moreover, the significant decline in hatching and survival rates observed in *S. prenanti* embryos and larvae underscored the detrimental impact of TDGS on early developmental stages. The detrimental effects of TDGS on the early development of *S. prenanti* were also evident in the observed reduction in body length and elevated heart rate.

The mechanisms underlying the observed effects of TDGS on *S. prenanti* may involve the combined effects of bubble formation and gas bubble disease, hypoxia and oxidative stress, physiological stress responses, and disruption of osmoregulation and nutrient utilization. Elevated TDGS levels facilitate the penetration of microbubbles through egg membranes, leading to their accumulation inside the eggs. This disrupts gas exchange and nutrient flow, impairing embryonic

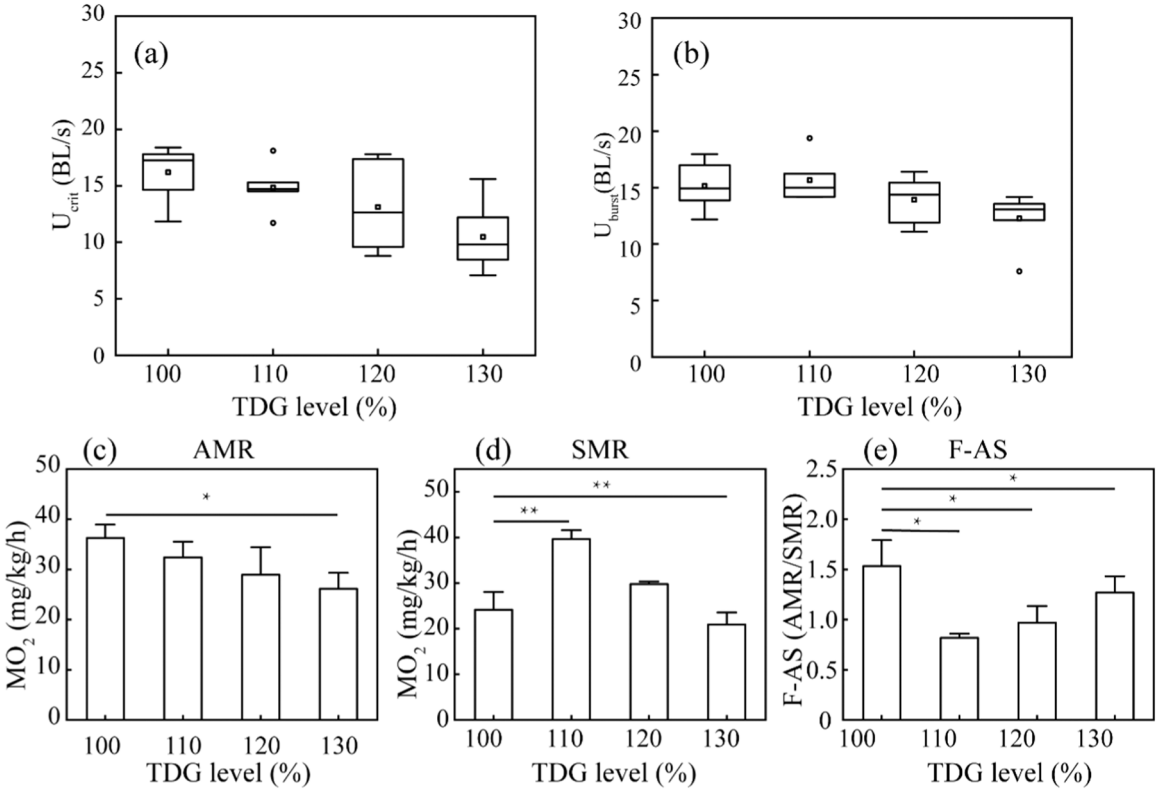

Fig. 5. Box plot representing (a) U_{crit} and (b) U_{burst} for juveniles exposed to varying TDGS levels for 35 h. The horizontal line within each box denotes the median, the boundaries of the rectangle correspond to the first and third quartiles, and the whiskers represent the range. Panels (c) AMR, (d) SMR, and (e) F-AS depict juveniles' metabolic rates under different TDGS levels for the same duration. n = 6. Asterisks denote the significance of the differences, with * and ** representing p-values less than 0.05 and 0.01, respectively.

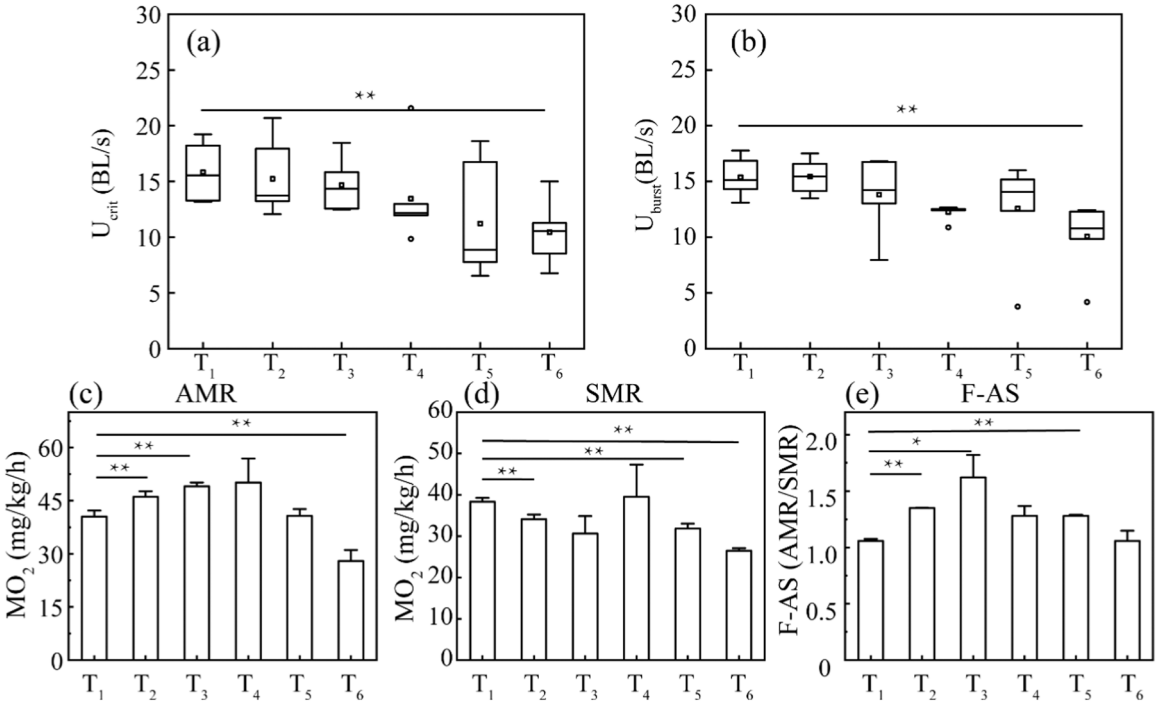

Fig. 6. Box plot of (a) U_{crit} and (b) U_{burst} for juvenile tested at various TDGS exposure durations in 130 % TDGS group. The horizontal line within the box represents the median, the ends of the rectangle indicate the first and third quartiles, and the whiskers depict the range. Panels (c) AMR (d) SMR (e) and F-AS for juvenile tested at various TDGS exposure durations in 130 % TDGS group. n = 6. Asterisks denote the significance of the differences, with * and ** representing p-values less than 0.05 and 0.01, respectively.

Table 3
Comparison of linear models for U_{crit} in juvenile fish exposed to different TDGS levels over varying durations and survival rates. Asterisks denote the significance of the differences, with *, **, and *** representing *p*-values less than 0.05, 0.01, and 0.001, respectively.

		Coefficient	SE	*t* value	*p*	AIC
Model 1	Intercept	15.73	5.50	2.86	**	313
	TDGS	3.78	4.42	−0.86		
Model 2	Intercept	19.01	4.74	4.01	***	295
	TDGS	−10.42	4.02	−2.59	*	
	Survival rate	7.57	1.61	4.69	***	
Model 3	Intercept	25.74	5.33	4.83	***	298
	TDGS	−8.95	4.04	−2.22	*	
	Duration	−0.69	0.16	−4.30	***	
Model 4	Intercept	19.26	6.62	2.91	**	297
	TDGS	−10.40	4.08	−2.55	*	
	Survival rate	7.33	4.56	1.61		
	Duration	−0.03	0.45	−0.06		

Table 4
Comparison of linear models for U_{burst} in juvenile fish exposed to different TDGS levels over varying durations and survival rates. Asterisks denote the significance of the differences, with *, **, and *** representing *p*-values less than 0.05, 0.01, and 0.001, respectively.

		Coefficient	SE	*t* value	*p*	AIC
Model 1	Intercept	13.898	3.481	3.99	***	260
	TDGS	−1.350	2.798	−0.48		
Model 2	Intercept	15.089	3.380	4.47	***	256
	TDGS	−3.765	2.871	−1.31		
	Survival rate	2.751	1.150	2.39	*	
Model 3	Intercept	17.522	3.740	4.69	***	257
	TDGS	−3.222	2.833	−1.14		
	Duration	−0.252	0.113	−2.22	*	
Model 4	Intercept	15.097	4.725	3.20	**	258
	TDGS	−3.764	2.912	−1.29		
	Survival rate	2.744	3.253	0.84		
	Duration	−0.001	0.318	0.00		

development and increasing mortality in chum salmon (Geist et al., 2013; Weitkamp and Katz, 1980). In terms of rainbow trout larvae, microbubbles can cause circulatory blockages and tissue damage within blood vessels, further impairing metabolism and survival (Schisler et al., 2000; Stroud et al., 1975). In chinook salmon and steelhead trout, the accumulation of bubbles in tissues and organs can lead to localized hypoxia, triggering oxidative stress and disrupting cellular homeostasis (Dawley and Ebel, 1975). Hypoxic conditions are known to induce developmental stress responses in fish, including the upregulation of stress hormones like cortisol, which can impair growth and survival (Pottinger, 2008). Elevated TDGS levels induce physiological stress, as evidenced by the marked increase in heart rate observed in *S. prenanti* larvae. This may result from elevated cortisol levels, which enhance basal metabolic rates and increase oxygen demand (Pottinger, 2008). Alternatively, in chinook salmon, circulatory blockages caused by microbubbles may force the heart to work harder to maintain adequate blood flow and oxygen delivery under hypoxic conditions (Gallaugher et al., 2001; Pleizier and Brauner, 2024). TDGS-induced bubble accumulation in tissues and organs may impair osmoregulation and nutrient absorption, leading to reduced growth rates. For instance, bubbles in the swim bladder can cause buoyancy imbalances in rainbow trout, impairing swimming behavior and feeding efficiency, which further exacerbates growth retardation (Shrimpton et al., 1990).

The adverse effects of TDGS on early development are consistent with findings in other species. For example, herring larvae experienced mortality due to excessive bubble accumulation in internal organs under TDGS conditions (Dannevig and Dannevig, 1950). Similarly, newly hatched trout larvae exhibited bubble formation on their surfaces, causing them to float and reducing their survival rates (Machado, 1984). In salmon larvae, bubbles formed between the yolk sac and the perivitelline membrane, leading to mortality upon yolk membrane rupture (Stroud et al., 1975). These findings highlight the widespread impact of TDGS on aquatic ecosystems and underscore the need for mitigation measures to protect vulnerable species.

The sensitivity to TDGS varies significantly among species, with *S. prenanti* exhibiting heightened vulnerability compared to others. For example, the *Myxocyprinus asiaticus* experienced a decrease in hatching rates from 78.3 % in the control group to 71.3 % at 130 % TDGS (Li et al., 2019), while *Schizothorax davidi* showed a reduction from 91.1 % to 69.2 % under similar conditions (Liang et al., 2013). In contrast, *S. prenanti* demonstrated a more pronounced decline in hatching rates (from 84 % to 58.7 %), suggesting greater sensitivity to TDGS-induced developmental damage. The observed differences in sensitivity may be linked to species-specific adaptive traits. For example, *Schizothorax davidi* may possess more efficient mechanisms for mitigating bubble formation or repairing tissue damage caused by TDGS, allowing it to maintain higher survival rates under similar conditions (Liang et al., 2013), while *S. prenanti* may lack such adaptations, making it more susceptible to TDGS-induced stress. Additionally, species with higher metabolic flexibility or enhanced antioxidant defenses may better withstand the oxidative stress associated with TDGS (Chen et al., 2023b, 2023c). Understanding these adaptive traits is crucial for predicting how different species will respond to changing environmental conditions and for developing targeted conservation strategies. The differences in sensitivity to TDGS among species have profound ecological implications. For instance, *S. prenanti*'s heightened vulnerability may place it at a competitive disadvantage in environments affected by TDGS, as reduced survival and growth rates could limit its ability to compete for resources with more tolerant species like the Chinese sucker. Additionally, impaired swimming behavior due to buoyancy issues may increase predation risk, further reducing its population viability in affected ecosystems (Shrimpton et al., 1990).

4.2. The effect of TDGS on the MO_2 and swimming performance of juveniles

AMR denotes the energy expenditure of fish during active states, reflecting the metabolic demands of high-intensity activities such as swimming, foraging, and evading predators (MacNutt, 2003). In terms of *S. prenanti*, exposure to a 130 % level of TDGS resulted in a significant decline in AMR, indicating that this TDGS level exceeded the species' metabolic regulation threshold. Notably, AMR initially increased but then decreased with prolonged exposure to 130 % TDGS, likely due to the heightened energy demands on muscles and tissues during swimming, leading to enhanced cardiac circulation and capillary expansion (Gallaugher et al., 2001). Additionally, the stress response triggered by TDGS, characterized by elevated heart rates, increased respiratory frequency, and other compensatory metabolic processes (Yuan et al., 2024), contributed to the early rise in AMR. However, with prolonged exposure, AMR declined as mortality rates increased, likely attributed to the accumulation of bubbles in tissues and the circulatory system. This accumulation impaired blood flow, reduced oxygen transport, and ultimately lowered metabolic efficiency (Pleizier and Brauner, 2024).

SMR, defined as the metabolic rate of resting, fasted fish at a specific temperature, encompasses the energy required for basic physiological functions, including stress responses (Beverton and Holt, 2012). In terms of *S. prenanti*, SMR was significantly elevated at 110 % TDGS compared to control conditions, likely reflecting an adaptive response to mild supersaturation. This response involves an increase in basal metabolic activity to regulate internal conditions and cope with TDGS-induced stress. However, at 130 % TDGS, a significant drop was observed in SMR, suggesting that this higher level of TDGS exceeded the organism's tolerance. This exceedance resulted in cellular damage, which impaired oxygen transport and disrupted metabolic pathways, thus reducing basal metabolic activity. Additionally, the progressive decline in SMR

fluctuations at 130 % TDGS indicates that prolonged exposure caused damage to the gills and heart of *S. prenanti* (Bulbul Ali and Mishra, 2022; Pleizier and Brauner, 2024), impairing respiratory and metabolic functions and eventually leading to a loss of survival capacity.

The swimming capacities of *S. prenanti* were notably affected by exposure to TDGS. U_{crit}, a measure of endurance swimming, primarily relies on oxygen consumption and aerobic metabolism, while U_{burst}, which reflects burst swimming, depends on the rapid mobilization of stored energy in muscles, such as ATP and phosphocreatine. Both U_{crit} and U_{burst} exhibited a downward trend with increasing TDGS levels and prolonged exposure times. However, significant reductions were only evident under conditions of extreme mortality (75 % mortality). These findings indicate that metabolic capacities, particularly SMR and AMR, are more sensitive to TDGS stress than swimming abilities, which experienced delayed but eventual declines under severe conditions. This lag in swimming performance decline may be attributed to the species' unique physiological adaptations, which support strong swimming performance despite early metabolic disruptions.

F-AS, the ratio of AMR to SMR, reflects the metabolic flexibility of fish when transitioning from rest to peak activity (Killen et al., 2007). A higher F-AS indicates greater adaptability to environmental stress and physical exertion. In this study, F-AS decreased as mortality rates increased, approaching a value of 1 at a 75 % mortality rate, which signifies a collapse in metabolic flexibility and adaptive capacity. The overall pattern of F-AS, initially increasing and then decreasing over exposure time, mirrors the trend observed in AMR, further reinforcing the conclusion that TDGS exerts a more pronounced impact on metabolic capacity than on swimming abilities. The delayed decline in swimming performance relative to metabolic changes implies that *S. prenanti* possesses physiological traits that temporarily buffer against the detrimental effects of TDGS on locomotion.

4.3. Applications

This study investigated the detrimental effects of TDGS on the developmental stages of *S. prenanti*, emphasizing the sensitivity of eggs, larvae, and juveniles. Understanding the differential impacts on these life stages is essential for evaluating population dynamics and survival risks for this species, particularly in dam-regulated river systems. Fish eggs, although partially shielded by their membranes and reliant on internal yolk reserves for nutrition, remain susceptible the external environment (Holt, 2011), particularly to stressors capable of penetrating these protective membranes. In contrast, larvae, being fully exposed to external conditions, show more pronounced physiological responses to TDGS stress. Juveniles possess fully developed organ systems and engage in critical life activities such as migration, foraging, and predator avoidance, all of which rely on their metabolic and swimming capabilities (Fisher and Leis, 2010). Impairment of these functions due to TDGS could indirectly elevate mortality risks. The study employed various indicators to investigate the characteristics of TDGS stress across these three developmental stages, as their distinct traits govern their sensitivity and responses to TDGS exposure.

Different species exhibit varying levels of tolerance to TDGS across developmental stages (Pleizier et al., 2020). Some species show increased tolerance with maturation, with the most severe damage observed during the larval and juvenile stages (Cornacchia and Colt, 1984; Dennison and Marchyshyn, 1973). Conversely, other species demonstrate decreasing tolerance from the egg stage to the juvenile stage (Krise and Herman, 1989; Weitkamp and Katz, 1980). It has been posited that the protective membrane of fish eggs may inhibit the penetration of small gas bubbles, thereby safeguarding developmental processes. In contrast, juveniles, with fully developed respiratory systems, are more prone to microbubble accumulation via respiration.

Our findings indicate that TDGS exerts a range of adverse effects on the eggs, larvae, and juveniles of *S. prenanti*, with no evidence suggesting that any particular developmental stage is more severely impacted. The observed reductions in hatching and survival rates imply that a decline in the number of newly hatched fry could precipitate a gradual decrease in population size. Additionally, the shortened body lengths and elevated heart rates in larvae indicate significant disruptions and damage to their growth, compromising their ability to maintain normal physiological functions or withstand environmental stressors. Furthermore, these larvae may encounter challenges in reproduction or heightened vulnerability to predation as they mature. Abnormal variations in both AMR and SMR resulting from TDGS reflect the impaired metabolic functions in juveniles, hindering their growth and development. The observed decline in both sustained and burst swimming abilities suggests that juveniles may struggle with effective foraging and predator evasion, potentially diminishing the overall survival rate of the population.

In conclusion, the findings of this study have significant implications for the management and conservation of aquatic ecosystems, particularly in regions affected by hydropower dam operations. The sensitivity of *S. prenanti* to TDGS highlights the need for targeted conservation strategies to mitigate the adverse effects of gas supersaturation on endemic fish populations. The results underscore the importance of regulating TDGS levels during flood seasons to protect vulnerable fish populations. Implementing measures such as controlled water releases from dams, aeration systems, or bubble curtains could help reduce TDGS levels in downstream habitats, thereby minimizing the risk of GBT and improving survival rates for sensitive species like *S. prenanti*. The study provides a scientific basis for developing regulatory guidelines that limit TDGS levels in rivers affected by hydropower operations. By establishing safe thresholds for TDGS, policymakers can ensure that dam operations do not compromise the health and sustainability of aquatic ecosystems. Furthermore, the findings can inform the development of regulatory guidelines and environmental assessments, promoting sustainable development that balances infrastructure needs with the preservation of aquatic biodiversity.

5. Conclusion

This study investigates the adverse effects of TDGS on *S. prenanti*, focusing on various parameters, including the survival rate, hatching rate, GBT rate of eggs, body length and heart rate of larvae, as well as the GBT probability, survival curves, swimming capacities (U_{crit}, U_{burst}), and metabolic rates (AMR, SMR, and F-AS) of juveniles. The research contributes to a deeper understanding of the negative impacts of TDGS across the developmental stages, from eggs, larvae, to juveniles. The main conclusions drawn from this study are as follows:

(1) Eggs incubated in water with TDGS levels exceeding 120 % exhibited significant GBT symptoms in both the eggs and the hatched larvae. Such elevated TDGS levels above 120 % substantially reduced the hatching and survival rates of *S. prenanti*, with higher TDGS levels correlating with lower rates.
(2) Larvae hatched in TDGS-rich water demonstrated significantly shorter body lengths at levels above 120 %, along with markedly increased heart rates at levels exceeding 110 %. These findings suggest potential developmental damage to internal organs resulting from TDGS exposure.
(3) Juveniles exposed to TDGS levels of 100 %, 110 %, 120 %, and 130 % exhibited a non-significant decreasing trend in both U_{crit} and U_{burst} as TDGS levels increased. However, those subjected to 130 % TDGS displayed significantly lower AMR, SMR, and F-AS compared to the control group, indicating that metabolic capacity is more susceptible to TDGS levels than swimming ability.
(4) Juveniles exposed to 130 % TDGS across different survival rates initially exhibited an increase in AMR, which subsequently decreased, while SMR fluctuated and declined with prolonged exposure. When survival rates reached 25 %, both U_{crit} and U_{burst} were significantly lower than those of the control group.

Additionally, AMR, SMR, and F-AS showed significant differences from the control group at a mortality rate of 50 %. These observations imply that metabolic capacity is more sensitive to the duration of TDGS exposure than swimming ability.

CRediT authorship contribution statement

Bo Zhu: Supervision. **Ruifeng Liang:** Software, Methodology. **Jun Du:** Methodology, Conceptualization. **Kefeng Li:** Supervision, Conceptualization. **Quan Yuan:** Writing – original draft. **wang yuanming:** Writing – review & editing, Supervision.

Ethics statement

The animal experimentation process has been approved by the Animal Experiment Ethics Committee of Sichuan University. All experimental procedures were carried out in accordance with the Experimental Animal Management Regulations endorsed by the State Council of the People's Republic of China.

Declaration of Competing Interest

The authors declare that they have no known competing financial interests or personal relationships that could have appeared to influence the work reported in this paper.

Acknowledgments

This work was supported by the National Natural Science Foundation of China (52209100 and 52179075), the Sichuan Natural Science Foundation (2024NSFSC0855) and the Open Fund Research at the Engineering Research Center of Eco-environment in Three Gorges Reservoir Region, Ministry of Education, China (KF2023-14).

Data availability

Data will be made available on request.

References

Arntzen, E.V., Hand, K.D., Carter, K.M., Geist, D.R., Murray, K.J., Dawley, E.M., Cullinan, V.I., Elston, R.A., Vavrinec, J., 2009. Total dissolved gas effects on incubating chum salmon below bonneville dam. Pacific Northwest National Lab. (PNNL). Richland, WA (United States).

Berg, A., 1992. Air entrainment and supersaturation of dissolved air in a shaft under atmospherical and reduced pressure conditions. J. Hydraul. Res. 30 (3), 327–340.

Beverton, R.J., Holt, S.J., 2012. On the dynamics of exploited fish populations. Springer Science & Business Media.

Brett, J.R., 1964. The respiratory metabolism and swimming performance of young sockeye salmon. J. Fish Res. Board Can. 21 (5), 1183–1226.

Bulbul Ali, A., Mishra, A., 2022. Effects of dissolved oxygen concentration on freshwater fish: a review. Int. J. Fish. Aquat. Stud. 10 (4), 113–127.

Chabot, D., Steffensen, J., Farrell, A., 2016. The determination of standard metabolic rate in fishes. J. Fish. Biol. 88 (1), 81–121.

Chen, Q., Li, Q., Lin, Y., Zhang, J., Xia, J., Ni, J., Cooke, S.J., Best, J., He, S., Feng, T., 2023a. River damming impacts on fish habitat and associated conservation measures. Rev. Geophys. 61 (4), e2023RG000819.

Chen, Y., Wu, X., Lai, J., Liu, Y., Song, M., Li, F., Gong, Q., 2023b. Integrated biochemical, transcriptomic and metabolomic analyses provide insight into heat stress response in Yangtze sturgeon (Acipenser dabryanus). Ecotoxicol. Environ. Saf. 249, 114366.

Chen, Y., Wu, X., Lai, J., Yan, B., Gong, Q., 2023c. Molecular mechanisms of physiological change under acute total dissolved gas supersaturation stress in yellow catfish (Pelteobagrus fulvidraco). Environ. Sci. Pollut. Res. 30 (43), 97911–97924.

Cornacchia, J., Colt, J., 1984. The effects of dissolved gas supersaturation on larval striped bass, morone saxatilis (Walbaum). J. Fish. Dis. 7 (1), 15–27.

Dannevig, A., Dannevig, G., 1950. Factors affecting the survival of fish larvae. ICES J. Mar. Sci. 16 (2), 211–215.

Dawley, E.M., Ebel, W.J., 1975. Effects of various concentrations of dissolved atmospheric gas on juvenile chinook salmon and steelhead trout. Fish. Bull. 73 (4). P 777-796, 1975. 4 FIG, 2 TAB, 18 REF.

Dennison, B.A., Marchyshyn, M.J., 1973. A device for alleviating supersaturation of gases in hatchery water supplies. Progress. Fish. Cult. 35 (1), 55–58.

Farrell, A., 2016. Pragmatic perspective on aerobic scope: peaking, plummeting, pejus and apportioning. J. Fish. Biol. 88 (1), 322–343.

Fisher, R., Leis, J.M., 2010. Swimming speeds in larval fishes: from escaping predators to the potential for long distance migration. Fish locomotion: An eco-ethological perspective 333–373.

Gallaugher, P., Thorarensen, H., Kiessling, A., Farrell, A., 2001. Effects of high intensity exercise training on cardiovascular function, oxygen uptake, internal oxygen transport and osmotic balance in chinook salmon (Oncorhynchus tshawytscha) during critical speed swimming. J. Exp. Biol. 204 (16), 2861–2872.

Geist, D.R., Linley, T.J., Cullinan, V., Deng, Z., 2013. The effects of total dissolved gas on chum salmon fry survival, growth, gas bubble disease, and seawater tolerance. North Am. J. Fish. Manag. 33 (1), 200–215.

Glover, D., DeVries, D., Wright, R., 2012. Effects of temperature, salinity and body size on routine metabolism of coastal largemouth bass micropterus salmoides. J. Fish. Biol. 81 (5), 1463–1478.

Grill, G., Lehner, B., Thieme, M., Geenen, B., Tickner, D., Antonelli, F., Babu, S., Borrelli, P., Cheng, L., Crochetiere, H., 2019. Mapping the world's free-flowing rivers. Nature 569 (7755), 215–221.

Hanna, S., Jutfelt, F. and Clark, T.D. 2021. Investigating the gill-oxygen limitation hypothesis in fishes: intraspecific scaling relationships of metabolic rate and gill surface area.

Holt, G.J., 2011. Larval fish nutrition. John Wiley & Sons.

Huang, Z., Li, H., 2024. Dams trigger exponential population declines of migratory fish. Sci. Adv. 10 (19) eadi6580.

Killen, S.S., Costa, I., Brown, J.A., Gamperl, A.K., 2007. Little left in the tank: metabolic scaling in marine teleosts and its implications for aerobic scope. Proc. R. Soc. B Biol. Sci. 274 (1608), 431–438.

Krise, W., Herman, R., 1989. Tolerance of lake trout, salvelinus namaycush (Walbaum), sac fry to dissolved gas supersaturation. J. Fish. Dis. 12 (3), 269–273.

Latrubesse, E.M., Arima, E.Y., Dunne, T., Park, E., Baker, V.R., d'Horta, F.M., Wight, C., Wittmann, F., Zuanon, J., Baker, P.A., 2017. Damming the rivers of the Amazon basin. Nature 546 (7658), 363–369.

Li, N., Fu, C., Zhang, J., Liu, X., Shi, X., Yang, Y., Shi, H., 2019. Hatching rate of Chinese sucker (Myxocyprinus asiaticus Bleeker) eggs exposed to total dissolved gas (TDG) supersaturation and the tolerance of juveniles to the interaction of TDG supersaturation and suspended sediment. Aquac. Res. 50 (7), 1876–1884.

Li, P., Zhu, D.Z., Li, R., Wang, Y., Crossman, J.A., Kuhn, W.L., 2022. Production of total dissolved gas supersaturation at hydropower facilities and its transport: a review. Water Res. 223, 119012.

Liang, R.-f, Li, B., Li, K.-f, Tuo, Y.-c, 2013. Effect of total dissolved gas supersaturated water on early life of David's schizothoracin (Schizothorax davidi). J. Zhejiang Univ. Sci. B 14 (7), 632–639.

Machado, J.P., 1984. Histopathologic study of rainbow trout fry with gas bubble disease. Michigan State University.

MacNutt, M.J., 2003. Effects of temperature on the repeat swimming performance, metabolic rates and swimming economy of salmonids (Oncorhynchus spp.). University of British Columbia.

Messina-Henríquez, S., Aguirre, Á., Brokordt, K., Flores, H., Oliva, M., Allen, P.J., Álvarez, C.A., 2022. Swimming performance and physiological responses of juvenile cojinoba seriolella violacea in hypoxic conditions. Aquaculture 548, 737560.

Mommsen, T.P., 1998. Growth and metabolism. The physiology of fishes 2, 65–97.

Pleizier, N.K., Algera, D., Cooke, S.J., Brauner, C.J., 2020. A meta-analysis of gas bubble trauma in fish. Fish Fish. 21 (6), 1175–1194.

Pleizier, N.K., Brauner, C.J., 2024. Causes and consequences of gas bubble trauma on fish gill function. J. Comp. Physiol. B 1–9.

Pottinger, T.G., 2008. The stress response in fish-mechanisms, effects and measurement. Fish. Welf. 32–48.

Pulg, U., Lennox, R.J., Enqvist, M., Stranzl, S.F., Espedal, E.O., Schwarz, M., Lorke, A., Flödl, P., Hauer, C., Schletterer, M., 2024. Assessing the potential for gas supersaturation downstream of hydropower plants in Norway, Austria and Germany. Sci. Total Environ. 948, 174645.

Pulg, U., Vollset, K.W., Velle, G., Stranzl, S., 2016. First observations of saturopeaking: characteristics and implications. Sci. Total Environ. 573, 1615–1621.

R Core Team. 2023. R: A Language and Environment for Statistical Computing. Vienna: R Foundation for Statistical Computing. https://www.R-project.org.

Sanches, P.V., Nakatani, K., Bialetzki, A., Baumgartner, G., Gomes, L.C., Luiz, E.A., 2006. Flow regulation by dams affecting ichthyoplankton: the case of the porto primavera dam, Paraná river, Brazil. River Res. Appl. 22 (5), 555–565.

Schisler, G.J., Bergersen, E.P., Walker, P.G., 2000. Effects of multiple stressors on morbidity and mortality of fingerling rainbow trout infected with myxobolus cerebralis. Trans. Am. Fish. Soc. 129 (3), 859–865.

Shrimpton, J., Randall, D., Fidler, L., 1990. Assessing the effects of positive buoyancy on rainbow trout (Oncorhynchus mykiss) held in gas supersaturated water. Can. J. Zool. 68 (5), 969–973.

Stroud, R.K., Bouck, G.R., Nebeker, A.V., 1975. Pathology of acute and chronic exposure of salmonid fishes to supersaturated water. Chemistry and physics of aqueous gas solutions 435–449.

Stuart, I.G., Sharpe, C.P., 2020. Riverine spawning, long distance larval drift, and floodplain recruitment of a pelagophilic fish: a case study of golden perch (Macquaria ambigua) in the arid Darling river, Australia. Aquat. Conserv. Mar. Freshw. Ecosyst. 30 (4), 675–690.

Wang, Y., Li, Y., An, R., Li, K., 2018. Effects of total dissolved gas supersaturation on the swimming performance of two endemic fish species in the upper Yangtze river. Sci. Rep. 8 (1), 10063.

Wang, H., Wang, Y., Li, K., Liang, R., Zhao, W., 2024. Tolerance threshold of a pelagic species in China to total dissolved gas supersaturation: from the perspective of survival characteristics and swimming ability. Conserv. Physiol. 12 (1), coae023.
Weitkamp, D.E., Katz, M., 1980. A review of dissolved gas supersaturation literature. Trans. Am. Fish. Soc. 109 (6), 659–702.
Yang, G., Bao, M., Cong, N., Kattel, G., Li, Y., Xi, Y., Wang, Y., Wang, Q., Yao, W., 2024. Application of a fish habitat model to assess habitat fragmentation using high flow and sediment transport in the rumei dam in lancang river (China). Ecohydrology 17 (4), e2583.
Yuan, Q., Zhang, Z., Li, K., Liang, R., Zhu, B., Wang, Y., 2024. Effect of total dissolved gas supersaturation on swimming performance of migratory fish for traversing velocity barriers. Aquac. Res. 2024 (1), 8846496.
Zhang, Q., Liu, X., Shi, H., Yang, Y., 2024. Interactive effects of total dissolved gas supersaturation and suspended sediment on the swimming abilities of two fish species. Ecol. Freshw. Fish. 33 (2), e12765.
Zhang, P., Qiao, Y., Grenouillet, G., Lek, S., Cai, L., Chang, J., 2021. Responses of spawning thermal suitability to climate change and hydropower operation for typical fishes below the three gorges dam. Ecol. Indic. 121, 107186.